9th National Congress on Civil Engineering, 10-11 May 2016
Ferdowsi University of Mashhad, Mashhad, Iran

Simulation of wave-induced motions of a moored floating breakwater using SPH method

Ehsan Delavari[1], Ahmad Reza Mostafa Gharabaghi[2]

1- Ph.D. Candidate, Faculty of Civil Engineering, Sahand University of Technology, Tabriz, Iran

2- Professor, Faculty of Civil Engineering, Sahand University of Technology, Tabriz, Iran

mgharabaghi@sut.ac.ir

Abstract

In this study, the dynamic motions of a rectangular chain-moored floating breakwater with three degrees of freedom (heave, sway, and roll motions) are simulated using a weakly-compressible smoothed particle hydrodynamic (WCSPH) scheme. A regular wave is simulated using a piston type wave maker inside a numerical wave flume. Then, a rectangular moored floating breakwater is placed inside the developed numerical wave flume and the dynamic motions of the structure are recorded. In the developed numerical scheme, the wave-structure and mooring-structure interactions are evaluated by solving new SPH-based equations. In addition, the mooring system is simulated by the SPH particles. Comparing the obtained results from the developed SPH scheme with the experimental data reveals that the modified smoothed-particle hydrodynamic scheme is able to simulate the dynamic motions of a chain-moored floating breakwater with a reasonable accuracy.

Keywords: Wave-structure interaction, Floating breakwater, Chain mooring, Regular wave, WCSPH.

1. INTRODUCTION

Floating breakwater as a special type of breakwater is used for attenuation of the wave effects. In these types of structures, forces exerted by the propagating waves on the structure cause it to move. These motions can also influence the wave characteristics and affect the stability of the structure. To reduce the wave-induced motions, the floating breakwaters are constrained by pile or cable/chain mooring systems.

In literature, there are several experimental as well as numerical studies on the performance of moored floating breakwaters. Yamamoto [1] investigated the response of moored floating breakwater due to regular as well as irregular waves theoretically and compared the results with experimental data. Williams and Abul-azm [2] studied the hydrodynamic properties of a dual pontoon floating breakwater consisting of a pair of floating cylinders with rectangular section, connected by a rigid deck, theoretically. Bhat [3] investigated experimentally and theoretically the performance of a rectangular and circular twin-pontoon floating breakwater. His hydrodynamic analysis was based on the linear potential theory which utilizes Green's theorem. Sannasiraj et al. [4] studied experimentally and numerically the behavior of a pontoon-type floating breakwater with three different mooring patterns. They used a two-dimensional finite element method for solving the potential-based equations. Williams et al. [5] investigated theoretically the hydrodynamic properties of a pair of long pontoon-type floating breakwaters using the boundary integral equation method. Bayram [6] conducted an experimental study to evaluate the performance of an inclined pontoon type breakwater under regular waves in intermediate water depths. Abul-Azm and Gesraha [7] examined theoretically the hydrodynamic properties and dynamic responses of a long floating pontoon-type floating breakwater. Lee and Cho [8] employed a boundary element method to solve the interaction between waves and a floating breakwater. In another work, a numerical investigation on a moored pontoon-type floating breakwater was carried out by Lee and Cho [9] using the element-free Galerkin method. Loukogeorgaki and Angelides [10] studied the performance of a moored floating breakwater under the action of normal incident waves in the frequency domain using a three-dimensional panel method utilizing Green's theorem. Rosales and Filipich [11] studied the dynamic behavior of a two-dimensional Catenary Anchor Leg Mooring (CALM) floating structure with a simplified SDOF equation using an algebraic recurrence algorithm. Rahman et al. [12] performed a numerical and experimental study to estimate the nonlinear dynamics of a pontoon type moored submerged floating breakwater under wave action and the forces acting on the mooring lines, for both the vertical and inclined mooring alignments. Martinelli et al. [13] examined the effect of floating breakwater layouts on wave transmission, loads along the moorings and connectors, under oblique waves, experimentally. Dong et al. [14] conducted two-dimensional physical model tests in a wave-current flume to measure the wave transmission coefficients of the three types of floating breakwaters with a single box, double box, and board nets, under regular waves with or without currents. Elchahal et al. [15] performed a parametric study on the behavior of a moored floating breakwater with a leeward boundary, assimilating the port quay walls, using a diffraction-radiation boundary value problem and investigated its motions. Diamantoulaki and Angelides [16, 17] investigated the overall performance of a free array of floating breakwaters connected by hinges and a cable-moored array of floating breakwaters connected by hinges under the action of monochromatic linear waves in the frequency domain. Peňa et al. [18] studied experimentally the efficiency of a floating breakwater by analyzing the hydrodynamic properties and mooring forces of floating breakwaters with four different designs. They concluded that the width of the pontoons is one of the key design parameters, while small modifications in the floating breakwater's cross section shape are less determinant in its hydrodynamic behavior and in mechanical loads. Chen et al. [19] studied the hydrodynamic behavior of a floating breakwater consisting of a rectangular pontoon and horizontal plates in time-domain, theoretically. He et al. [20, 21] investigated experimentally the hydrodynamic performance of floating breakwaters with symmetric and asymmetric pneumatic chambers. In another work, Koraim and Rageh [22] studied the hydrodynamic efficiency of a floating breakwater using physical models. Loukogeorgaki et al. [23] performed 3D experiments to investigate the structural response and the efficiency of a floating breakwater with flexibly connectors and moored with chains under the action of perpendicular and oblique regular and irregular waves.

Most of the numerical methods applied for the investigation of the response of floating breakwaters are generally based on potential flow theory. This is due to the complexity of problems dealing with the wave-structure interaction. Solving these problems using potential theory based methods need some simplifying assumptions that can affect the accuracy of the results. Currently, in order to reduce these deficiencies, some simple solver methods for Navier-Stokes' equations such as Smoothed Particle Hydrodynamic (SPH) scheme have been developed. Manenti and Ruol [24] studied the dynamic response of a pile-moored floating breakwater as a case study for fluid-structure interaction using the SPH method. They used a weakly-compressible SPH scheme for calculating the heave motion of the structure under regular wave action. Recently, Duran [25] applied the SPH method for optimizing the performance of a floating breakwater with a practical application. There are very limited studies performed on the behavior of chain-moored floating breakwater using the SPH scheme.

In this paper, the performance of a pontoon-type chain-moored floating breakwater under the regular wave action is investigated using the modified SPH scheme. In the modified scheme, the SPH particles for simulating the mooring system were used. For this purpose, the dynamic responses of the structure for heave, sway, and roll motions are estimated. The obtained results are compared with the experimental data to evaluate the efficiency of the modified SPH method in simulating the behavior of a chain-moored floating breakwater.

2. WEAKLY-COMPRESSIBLE SPH SCHEME

For simulation of a weakly-compressible, viscous fluid, the well-known Navier-Stokes equations were solved. These equations can be written in a Lagrangian form as:

$$\frac{d\rho}{dt} = -\rho \nabla \cdot \vec{u} \tag{1}$$

$$\frac{d\vec{u}}{dt} = -\frac{1}{\rho}\nabla p + \nu \nabla^2 \vec{u} + \vec{g} \tag{2}$$

where $\vec{u}$ is the fluid velocity vector, ρ is the fluid density, p is the pressure, $\vec{g}$ is the body force vector (e.g. gravity force) and ν is the kinematic viscosity considered as equal to $1\times10^{-6}\, m^2/s$. In the SPH scheme, the fluid domain is discretized as a finite number of particles. Each of these particles represents a small volume of the fluid domain having its own physical properties. For particle *i*, the discretized SPH form of the governing equations can be written, by exerting a summation on the neighboring particles *j*, as:

$$\frac{D\rho_i}{Dt} = \sum_{j=1}^{N} m_j \left(\vec{u}_i - \vec{u}_j\right)\cdot \nabla_i W_{ij} \tag{3}$$

$$\frac{D\vec{u}_i}{Dt} = -\sum_{j=1}^{N} m_j \left(\frac{p_i}{\rho_i^2} + \frac{p_j}{\rho_j^2} + R\left(f_{ij}\right)^4 \right) \nabla_i W_{ij} + \nu\left(\nabla^2 \vec{u}\right)_i + \vec{g}_i \quad (4)$$

Also:

$$\frac{D\vec{r}_i}{Dt} = \vec{u}_i \quad (5)$$

In these equations, m is the mass, $\vec{r}$ is the position vector, and W is a smoothing kernel function. In this paper, the cubic spline kernel was used as the kernel function which is given by [26]:

$$W(q,h) = \alpha_d \begin{cases} 1 - \frac{3}{2}q^2 + \frac{3}{4}q^3, 0 \le q \le 1 \\ \frac{1}{4}(2-q)^3, 1 \le q \le 2 \\ 0, q \ge 2 \end{cases} \quad (6)$$

where $q = r/h$, h is the smoothing length of the kernel function, r is the distance between the particles i and j and $\alpha_d = 10/\pi h^2$. Term $R(f_{ij})^4$ in equation (4) is the artificial pressure term introduced by Monaghan to remove the tensile instability problem. For more details, see reference [27].

A density re-initialization technique was used by applying a zero order Shepard filter on the density field every 20 time steps in order to reduce the artificial density fluctuations. It can be written as [28]:

$$\rho_i^{new} = \sum_{j=1}^{N} m_j \widetilde{W}_{ij} \quad (7)$$

in which:

$$\widetilde{W}_{ij} = W_{ij} / \sum_j W_{ij} \frac{m_j}{\rho_j} \quad (8)$$

In the WCSPH scheme, the pressure field is calculated by an equation of state relating the density field directly to the pressure field. To impose the weakly-compressibility, a numerical speed of sound c_0 is introduced which is usually at least ten times larger than the maximum velocity of the fluid in the flow field. The magnitude of this parameter is very lower than its real value and is chosen in such a way that ensures the fluid density variations less than one percent in the flow field. The equation of state has been introduced by Monaghan [29] as:

$$p = \frac{c_0^2 \rho_0}{7}\left[\left(\frac{\rho}{\rho_0}\right)^7 - 1\right] \quad (9)$$

where ρ_0 is the reference density (here, $\rho_0 = 1000\ kg/m^3$).

To calculate the viscous force term in equation (4), the equation introduced by Lo and Shao [30] was used:

$$\nu\left(\nabla^2 u\right)_i = \sum_j m_j \frac{4(\mu_i + \mu_j)}{(\rho_i + \rho_j)^2} \frac{\vec{r}_{ij} \cdot \nabla_i W_{ij}}{r_{ij}^2 + \eta^2} \vec{u}_{ij} \quad (10)$$

where μ is the dynamic viscosity of the fluid, $\vec{r}$ is the position vector, $\vec{r}_{ij} = \vec{r}_i - \vec{r}_j$, $\vec{u}_{ij} = \vec{u}_i - \vec{u}_j$ and $\eta = 0.1h$.

3. WAVE-STRUCTURE INTERACTION

The solid dynamics is simulated by the second law of Newton. Linear and angular momentum equations are given in two-dimensional framework as:

$$M\frac{d\vec{V}_g}{dt} = M\vec{g} + \vec{F}_{fluid-body} \quad (11)$$

$$I_g \frac{d\Omega_g}{dt} = \vec{k} \cdot \vec{T}_{fluid-body} \quad (12)$$

where $\vec{V}_g$ and Ω_g are the velocity vector and the angular velocity of the center of gravity of the studied body, M and I_g are the mass and the moment of inertia of the body with respect to its center of gravity.

$\vec{F}_{fluid-body}$ and $\vec{T}_{fluid-body}$ are the vectors of fluid-body hydrodynamic force and torque, respectively, and $\vec{k}$ is the unit vector normal to the xz-plane.

There are different methods for calculating the hydrodynamic forces while using SPH scheme. One of the most common methods is proposed by Monaghan and Kajtar in the form of the following equations [31]:

$$\vec{F}_i = \sum_b m_b \left[\sum_i \left(\vec{f}_{bi} - \nu\left(\nabla^2\vec{u}\right)_b\right)\right] \tag{13}$$

in which:

$$\vec{f}_{bi} = \frac{\alpha}{\beta}\frac{\vec{r}_{bi}}{\left(r_{bi} - \dfrac{dp}{\beta}\right)^2} K\left(r_{bi}/h\right)\frac{2m_i}{m_b + m_i} \tag{14}$$

In these relations, subscript *i* and *b* are related to the fluid and solid particles, respectively, *dp* is the initial particle spacing, β is ratio of the solid particles' spacing to the fluid particles' spacing, and α is a constant and its value depends on the maximum velocity of fluid in the computational domain, $\nu(\nabla^2\vec{u})_b$ is the viscous force given by equation (10), $\vec{f}_{bi}$ is the force on solid particle *b* due to the fluid particle *i* and $K(r_{bi}/h)$ is a 1D kernel function. In this paper, the Wendland 1D quantic function is used which is given as [31]:

$$K(q) = \begin{cases} w_5(1 + \frac{5}{2}q + 2q^2)(2-q)^5, 0 \le q \le 2 \\ 0, q \ge 2 \end{cases} \tag{15}$$

where w_5 is a constant.

By precise concern of the Monaghan and Kajtar's equations, it can be shown that the inertia effects of solid particles' relative acceleration have not been considered. Therefore, in this paper, an additional term is added to the original equation (14) in order to consider the inertia effects due to the relative acceleration of the particles related to the structure due to its relative movements. The modified equation is given as:

$$\vec{f}_{bi} = \frac{\alpha}{\beta}\frac{\vec{r}_{bi}}{\left(r_{bi} - \dfrac{dp}{\beta}\right)^2} K\left(r_{bi}/h\right)\frac{2m_i}{m_b + m_i} + (\vec{g} - \vec{a}_i)W_{bi}\frac{m_i}{\rho_i} \tag{16}$$

On the other hand, in this study, the value of α related to the first term is considered different in *x* and *z* directions. This is due to the differences in the velocities of the fluid in *x* and *z* directions in wave domain. Therefore, it can be written as:

$$\alpha_x = \varphi\alpha_z \tag{17}$$

where φ is considered to be constant and $\varphi \ge 1$.

4. MOORING-STRUCTURE INTERACTION

Simulation of the mooring systems is one of the main challenges in SPH scheme. It is common to simulate the mooring system using finite element method and combine it with a SPH scheme using a contact algorithm. In this paper, for the first time, it is tried to simulate the chain-mooring system using the SPH scheme.

The mooring system has been simulated by four elastic solid rods on two sides of the structure. Stress components of an elastic body, can be written as [32]:

$$\sigma_{ij} = -P\delta_{ij} + S_{ij} \tag{18}$$

where *P* is the isotropic pressure, S_{ij} is the component of deviatoric stress tensor, and δ_{ij} is croneker delta. The rate of change of S_{ij} is given by:

$$\frac{DS_{ij}}{Dt} = 2\mu_s(D_{ij} - \frac{1}{3}D_{mm}\delta_{ij}) + S_{ik}\omega_{jk} + S_{kj}\omega_{ik} \tag{19}$$

where μ_s is the shear modulus, D_{ij} is the component of the rate of deformation tensor, and ω_{ij} is the component of the rate of rotational tensor. They can be written as:

$$D_{ij} = \frac{1}{2}\left(\frac{\partial v_i}{\partial x_j} + \frac{\partial v_j}{\partial x_i}\right) \tag{20}$$

$$\omega_{ij} = \frac{1}{2}\left(\frac{\partial v_i}{\partial x_j} - \frac{\partial v_j}{\partial x_i}\right) \tag{21}$$

After the SPH discretization, the governing equations for simulation of the mooring SPH particle *a* are given, by exerting a summation on the neighboring particles *b*, as:

$$\frac{D\rho_a}{Dt} = \sum_{b=1}^{N} m_b\left(\vec{u}_a - \vec{u}_b\right)\cdot\nabla_a W_{ab} \tag{22}$$

$$\frac{Du_{ai}}{Dt} = \sum_{b=1}^{N} m_b\left(\frac{\sigma_{ija}}{\rho_a^2} + \frac{\sigma_{ijb}}{\rho_b^2}\right)\frac{\partial W_{ab}}{\partial_a x_j} + \vec{g}_i \tag{23}$$

According to the equations proposed by Bui et al. [33], an equation for calculating the mooring forces due to its interaction with the structure was developed. This force is added to the right side of the equation (11). The proposed equation is given as:

$$f_{ai}^{n} = \begin{cases} -K_{ai}\vec{\delta}_n - c_n\vec{v}_{ai}^{\,n}, 2d_{ai} \le (h_a + h_i) \\ 0, 2d_{ai} \ge (h_a + h_i) \end{cases} \tag{24}$$

where d_{ai} is the distance between the particles of the mooring system *a* and structure particles *i*. h_a and h_i are the smoothing lengths of mooring particles and structure particles, respectively. K_{ai}^{n} is the stiffness of the mooring system in *n* direction, and c_n is the damping coefficient that is given by:

$$c_n = \zeta\sqrt{m_{ai}K_{ai}^{n}} \tag{25}$$

in which:

$$m_{ai} = \frac{m_a M_k}{m_a + M_k} \tag{26}$$

where ζ is the damping ratio, m_a is the mass of mooring particles, and M_k is the total mass of the floating structure.

$\vec{\delta}_n$ and $\vec{v}_{ai}^{\,n}$ are relative displacement and velocity between the mooring system and structure particles, respectively. $\vec{\delta}_n$ can be written as:

$$\delta_n = \vec{v}_{ai}^{\,n}\cdot dt \tag{27}$$

For calculating stiffness of the mooring system in *x* and *z* directions, the mooring analysis method proposed by Jingwall [34] was used. The method is based on the catenary equations and it needs an iterative procedure. For more details, refer to [34].

4. SIMULATION OF FLOATING BREAKWATER

According to an experimental study performed by He et al. [20], a rectangular moored-floating breakwater was placed into a wave flume with a water depth of 0.45 *m*. The breakwater is 0.75 *m* in width and 0.4 *m* in height. A regular wave, produced by a piston wave maker, impacts on the structure and causes it to move with three degrees of freedom (heave, sway, and roll). The height of the target wave is 0.04 *m*. six ratios of width of the breakwater (*B*) to incident wave length (*L*) have been considered. The period of the simulated waves ranged between 1.1 *s* to 2 *s* and the corresponding wave lengths from 1.75 *m* to 3.88 *m*. At the far end of the wave flume a sponge layer [35] with a length equal to the incident wave length is placed (Figure. 1). Depending on the length of the wave flume, the particle spacing is selected as 0.0085 *m*, 0.01 *m*, and/or 0.015 *m* and the fourth order Runge-Kutta scheme is used as a numerical integrator.

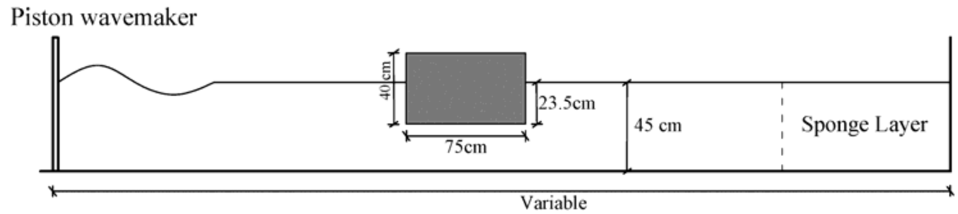

Figure 1. Schematic sketch of the numerical wave flume

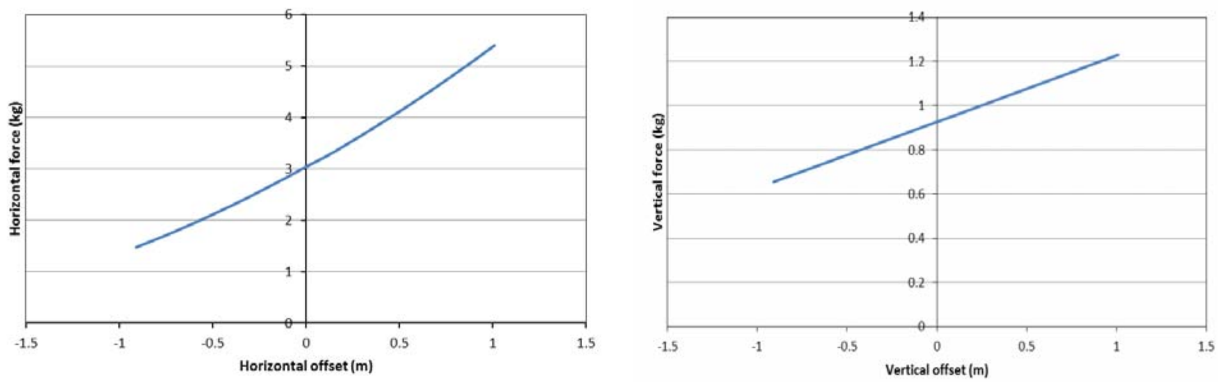

(a) **(b)**

Figure 2. Variations of a) the horizontal force vs. horizontal displacement, b) vertical force vs. vertical displacement for calculating the mooring stiffness in *x* and *z* directions

In Figure. 2, the results obtained from the mooring analysis in *x* and *z* directions are presented. As expected, variations of the horizontal force vs. horizontal displacement are nonlinear. Due to its little curvature, in this study, it is assumed to be linear.

Dynamic responses of moored floating breakwater are shown in Figure. 3. As can be seen, in all of three figures, maximum differences with the experimental data belong to the peak zones. Among these three figures, the best result belongs to the heave response with *B/L=0.193*. The error value is 0.68 percent. The worst result belongs to the heave response with *B/L=0.219* that its error value is 24.7 percent. As can be seen, behavior of the breakwater has changed with larger values than *B/L=0.219* and the proposed SPH model can nearly simulate it. As a result, it seems that the developed model can simulate wave-induced motions of the moored-floating breakwater with a reasonable accuracy. Of course, that was the first try in this field and it is obvious that it needs more study.

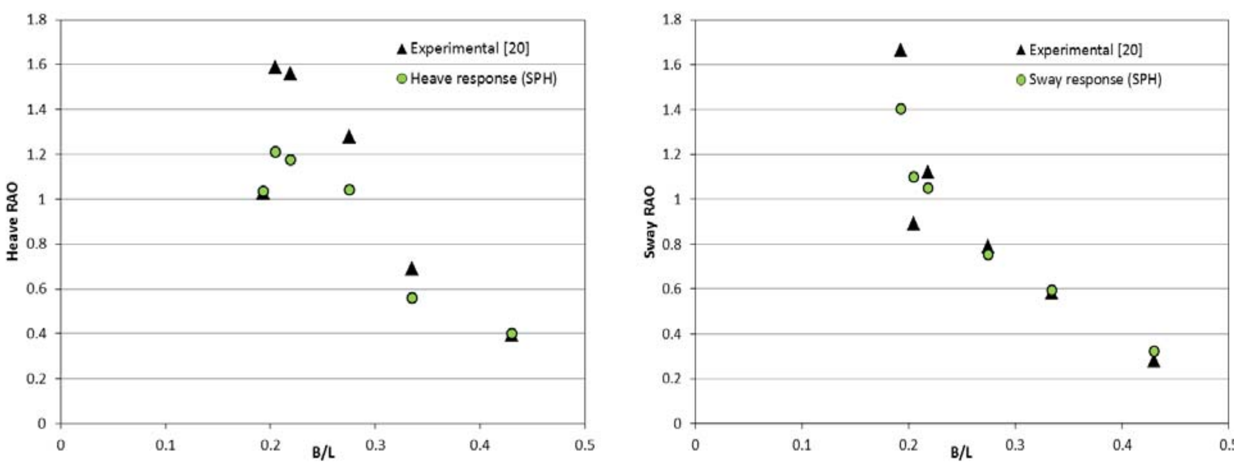

(a) **(b)**

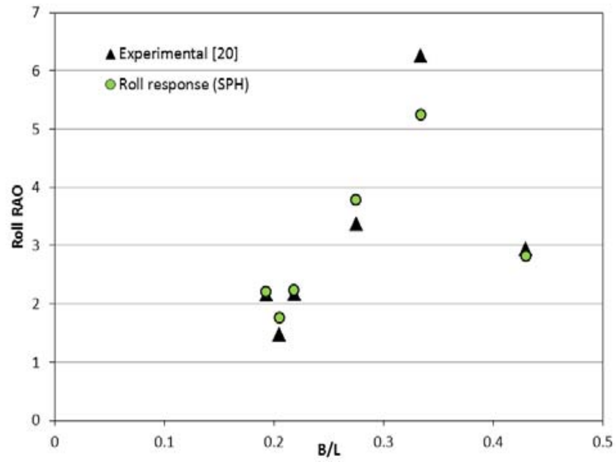

(c)

Figure 3. RAOs of the moored-floating breakwater for various ratios of *B*/*L*. a) heave, b) sway, c) roll.

5. Conclusions

A new SPH algorithm was proposed to simulate wave-structure and mooring-structure interactions induced by regular waves. To verify the proposed SPH scheme, a rectangular moored-floating breakwater, with three degrees of freedom, was placed into a wave flume and its dynamic responses in heave, sway, and roll motions were calculated. An investigation on the obtained results reveals that the proposed SPH scheme can simulate behavior of the floating breakwater with a reasonable accuracy and is reliable.

6. References

1. Yamamoto, T. (1981), "Moored floating breakwater response to regular and irregular waves," Applied Ocean Research, **3** (1), pp. 27-36.
2. Williams, A.N., and Abul-Azm, A.G. (1997), "Dual pontoon floating breakwater," Ocean Engineering, **24** (3), pp. 465-478.
3. Bhat, S.S. (1998), "*Performance of twin pontoon floating breakwaters*", Ph.D. Thesis, University of British Colombia.
4. Sannasiraj, S.A., Sundar, V., and Sundaravadivelu, R. (1998), "Mooring forces and motion responses of pontoon-type floating breakwaters," Ocean Engineering, **25** (1), pp. 27-48.
5. Williams, A.N., Lee, H.S., and Huang, Z. (2000), "Floating pontoon breakwaters," Ocean Engineering, 27, pp. 221-240.
6. Bayram, A. (2000), "Experimental study of a sloping float breakwater," Ocean Engineering, 27, pp. 445-453.
7. Abul-Azm, A.G., and Gesraha, M.R. (2000), "Approximation to the hydrodynamics of floating pontoons under oblique waves," Ocean Engineering, 27, pp. 365-384.
8. Lee, J., and Cho, W. (2002), "Effects of mean wave force on mooring tension and performance of a moored floating breakwater," KSCE Journal of Civil Engineering, **6** (2), pp. 193-201.
9. Lee, J., and Cho, W. (2003), "Hydrodynamic analysis of wave interactions with a moored floating breakwater using the element-free Galerkin method," Canadian Journal of Civil Engineering, 30, pp. 720-733.
10. Loukogeorgaki, E., and Angelides, D.C. (2005), "Stiffness of mooring lines and performance of floating breakwater in three dimensions," Applied Ocean Research, 27, pp. 187-208.
11. Rosales, M.B., and Filipich, C.P. (2006), "Full modeling of the mooring non-linearity in two-dimensional floating structure," International Journal of Non-Linear Mechanic, 41, pp. 1-17.
12. Rahman, Md. A., Mizutani, N., and Kawasaki, K. (2006), "Numerical modeling of dynamic responses and mooring forces of submerged floating breakwater," Coastal Engineering, 53, pp. 799-815.

13. Martinelli, L., Ruol, P., and Zanuttigh, B. (2008), "Wave basin experiments on floating breakwaters with different layouts," Applied Ocean Research, 30, pp. 199-207.
14. Dong, G.H., Zheng, Y.N., Li, Y.C., Teng, B., Guan, C.T., and Lin, D.F. (2008), "Experiments on wave transmission coefficients of floating breakwaters," Ocean Engineering, 35, pp. 931- 938.
15. Elchahal, G., Younes, R., and Lafon, P. (2009), "Parametrical and motion analysis of a moored rectangular floating breakwater." Journal of Offshore Mechanic and Arctic Engineering, 131, pp. 1-11.
16. Diamantoulaki, I., and Angelides, D.C. (2010), "Analysis of performance of hinged floating breakwaters." Eng. Struct., 32, pp. 2407-2423.
17. Diamantoulaki, I., and Angelides, D.C. (2011), "Modeling of cable-moored floating breakwaters connected with hinges," Eng. Struct., 33, pp. 1536-1552.
18. Peňa, E., Ferreras, J., and Sanchez-Tembleque, F. (2011), "Experimental study on wave transmission coefficient, mooring lines and module connector forces with different designs of floating breakwaters," Ocean Engineering, 38, pp. 1150-1160.
19. Chen, Z., Wang, Y., Dong, H., and Zheng, B. (2012), "Time-domain hydrodynamic analysis of pontoon-plate floating breakwater," Water Sci. Eng., **5** (3), pp. 291-303.
20. He, F., Huang, Z., and Law, A.W.K (2012), "Hydrodynamic performance of a rectangular floating breakwater with and without pneumatic chambers: An experimental study," Ocean Engineering, 53, pp. 16-27.
21. He, F., Huang, Z., and Law, A.W.K. (2013), "An experimental study of a floating breakwater with asymmetric pneumatic chambers for wave energy extraction," Appl. Energy, 106, pp. 222-231.
22. Koraim, A.S., and Rageh, O.S. (2013), "Effect of under connected plates on the hydrodynamic efficiency of the floating breakwater," China Ocean Engineering, **28** (3), pp. 349-362.
23. Loukogeorgaki, E., Yagci, O., and Kabdasli, M.S. (2014), "3D experimental investigation of the structural response and the effectiveness of a moored floating breakwater with flexibly connected modules," Coastal Engineering, 91, pp. 164-180.
24. Manenti, S., and Ruol, P. (2008), "Fluid-structure interaction in design of offshore wind turbines: SPH modeling of basic aspects," Proc., Handling Exceptions in Structural Eng. Conf., Rome.
25. Duran, D.A.R. (2013), "*Performance optimization of a floating breakwater model using SPH method, with a practical application*", Master Thesis, University of Las Palmas De Gran Canaria.
26. Monaghan, J.J. and Lattanzio, J.C. (1985), "A refined particle method for astrophysical problems," Astronomy and Astrophysics, **149**, pp. 135-143.
27. Monaghan, J.J. (2000), "SPH without a tensile instability," Journal of Computational Physics, **159**, pp. 290-311.
28. Gomez-Gesteria, M., Rogers, B.D., Crespo, A.J.C., Dalrymple, R.A., Narayanaswamy, M. and Dominguez, J.M. (2012), "SPHysics-Development of a free surface fluid solver-part 1: Theory and formulations," Computer and Geosciences, **48**, pp. 289-299.
29. Monaghan, J.J. (1994), "Simulating free surface flows with SPH," Journal of Computational Physics, **110**, pp. 399-406.
30. Monaghan, J.J. (1994), "Simulating free surface flows with SPH," Journal of Computational Physics, **110**, pp. 399-406.
31. Monaghan, J.J., and Kajtar, J.B. (2009), "SPH particle boundary forces for arbitrary boundaries," Computer Physics Communications, **180**, pp. 1811-1820.
32. Amini, Y., Emdad. H., and Farid, M. (2011), "A new model to solve fluid-hypo-elastic solid interaction using the smoothed particle hydrodynamics (SPH) method," European Journal of Mechanics B/Fluids, **30**, pp. 184-194.
33. Bui, H.H., Kodikara, J.K., Bouazza, A., Haque, A., and Ranjith, P. (2014), "A novel computational approach for large deformation and post-failure analysis of segmental retaining wall systems," International Journal for Numerical and Analytical Methods in Geomechanics, **38**, pp. 1321-1340.
34. Jingwall, J.R. (1997), "*The design of a deep water catenary riser*," Ph.D. Thesis, University of Glasgow.
35. Delavari, E., and Gharabaghi, A.R.M. (2014), "A modified sponge layer boundary condition for a numerical wave flume based on the SPH scheme." The 11th Int. Conf. on Coasts, Ports and Marine Structures (ICOPMAS 2014), Tehran.